Biochemical and Biophysical Research Communications 507 (2018) 304–310

Contents lists available at ScienceDirect

Biochemical and Biophysical Research Communications

journal homepage: www.elsevier.com/locate/ybbrc

Chemoattractant receptors activate, recruit and capture G proteins for wide range chemotaxis

Yukihiro Miyanaga [a], Yoichiro Kamimura [b], Hidekazu Kuwayama [c], Peter N. Devreotes [d], Masahiro Ueda [a, b, *]

[a] Laboratory for Single Molecular Biology, Graduate School of Frontier Biosciences, Osaka University, Suita, Osaka, 565-0871, Japan
[b] Laboratory for Cell Signaling Dynamics, Center for Biosystems Dynamics Research, RIKEN, Suita, Osaka, 565-0874, Japan
[c] Graduate School of Life and Environmental Sciences, University of Tsukuba, Japan
[d] Department of Cell Biology, Johns Hopkins University School of Medicine, 725 N. Wolfe St., 114 WBSB, Baltimore, MD, 21205, USA

ARTICLE INFO

Article history:
Received 22 October 2018
Received in revised form
1 November 2018
Accepted 5 November 2018
Available online 17 November 2018

Keywords:
Eukaryotic chemotaxis
Gradient sensing
Dynamic range extension
G protein-coupled receptor
Single-molecule analysis

ABSTRACT

The wide range sensing of extracellular signals is a common feature of various sensory cells. Eukaryotic chemotactic cells driven by GPCRs and their cognate G proteins are one example. This system endows the cells directional motility towards their destination over long distances. There are several mechanisms to achieve the long dynamic range, including negative regulation of the receptors upon ligand interaction and spatial regulation of G proteins, as we found recently. However, these mechanisms are insufficient to explain the 10^5-fold range of chemotaxis seen in *Dictyostelium*. Here, we reveal that the receptor-mediated activation, recruitment, and capturing of G proteins mediate chemotactic signaling at the lower, middle and higher concentration ranges, respectively. These multiple mechanisms of G protein dynamics can successfully cover distinct ranges of ligand concentrations, resulting in seamless and broad chemotaxis. Furthermore, single-molecule imaging analysis showed that the activated Gα subunit forms an unconventional complex with the agonist-bound receptor. This complex formation of GPCR-Gα increased the membrane-binding time of individual Gα molecules and therefore resulted in the local accumulation of Gα. Our findings provide an additional chemotactic dynamic range mechanism in which multiple G protein dynamics positively contribute to the production of gradient information.

1. Introduction

Chemotactic cells can sense chemical gradients over a wide range of background concentrations in various cell types, including bacteria and mammalian leukocytes, and is a common feature shared with other sensory cells [1,2]. The underlying mechanisms for the wide range sensitivity are negative feedback on the receptors and other signaling machinery [3–7]. A prolonged stimulation decreases the signaling ability of cells through the chemical modification, down-regulation, and signaling suppression of the receptors [3–7]. Suppressing the receptors and of the corresponding signaling pathways allows the cells to reset themselves so as to be less sensitive to the same level of signal inputs [3–7]. Thus, cells adapt to the absolute concentration of extracellular chemoattractant while still responding to changes. In *Dictyostelium discoideum* cells, the G protein-coupled chemoattractant receptor, cAR1, and the Gα2 and Gβγ subunits of the cognate G protein are involved in the gradient detection of extracellular cAMP, which can transduce chemotactic signals over a 10^5–10^6-fold range [8–10]. Upon cAMP stimulation, cAR1 is phosphorylated, which lowers its affinity for cAMP. Although receptor phosphorylation can contribute to extending the range of sensitivity, non-phosphorylated mutant cAR1-expressing cells still show chemotaxis over a 10^4-fold range [11,12].

We recently found an additional but essential mechanism for the range regulation that functions on the cognate G protein in *Dictyostelium* cells [13]. A G protein-binding protein named Gip1 can bind and sequester heterotrimeric Gα2Gβγ proteins in cytosolic

Abbreviations: Gip1, G protein-interacting protein 1; TMR, tetramethylrhodamine; TIRFM, total internal reflection fluorescence microscopy; SRD, short-range diffusion; PDF, probability density function; EL2, second extracellular loop; cAR1-R2(EL2), chimera receptor in which the second extracellular loop was replaced with that of cAR2, a low-affinity homolog of cAR1.

* Corresponding author. Graduate School of Frontier Biosciences, Osaka University, Suita, Osaka, 565-0871, Japan.
E-mail address: masahiroueda@fbs.osaka-u.ac.jp (M. Ueda).

https://doi.org/10.1016/j.bbrc.2018.11.029

pools and regulate the recruitment of trimeric G protein to the plasma membrane upon receptor activation, thus supplying more G protein for receptor-mediated signaling at middle ranges. Gip1-deficient cells can only show chemotaxis at lower concentrations even though the receptor phosphorylation is normal. However, additional mechanisms are expected to contribute to the range regulation in cells, because the Gip1-dependent translocation of G protein has an EC_{50} of about 10 nM, which can cover only a limited cAMP concentration range of chemotactxis [13]. In fact, *Dictyostelium* cells can exhibit chemotaxis at much higher cAMP concentrations (over 1 μM).

In the present study, we sought these additional mechanisms to understand how G protein transduces chemotactic signals over a wider range of chemoattractant concentrations. We consistently characterized the dynamics of G proteins upon cAMP stimulation by observing their activation, translocation, and molecular behaviors on the plasma membrane. We especially investigated the intracellular dynamics of G protein signaling using single-molecule imaging in living *Dictyostelium* cells, which allowed us to directly observe G protein behaviors on the membrane, which demonstrated unconventional coupling between cAMP-occupied cAR1 and activated Gα2. Unexpectedly, the G protein dynamics was regulated by distinct ligand signaling with EC_{50} of 2.3, 12 and 270 nM for activation, translocation, and unconventional coupling to the receptors. Moreover, lowering the affinity of cAR1 receptors was followed by concomitant changes in the EC_{50} of the unconventional coupling between cAR1 and activated Gα2, which further extended the chemotactic dynamic range. These studies provide an additional layer of chemotactic dynamic range regulation in which multiple types of G proteins dynamics positively contribute to the production of gradient information.

2. Materials and methods

2.1. Single-molecule microscopy

Single molecules were visualized using an objective type total internal reflection fluorescence microscope (TIRFM) constructed on an inverted fluorescence microscope (Olympus IX-70, PlanApo 60 × 1.45-NA oil objective; Nikon TE2000, Apo TIRF 60 × 1.49-NA oil objective), as described previously [14–18]. Fluorescence signals from TMR were intensified with an image intensifier (GaAsP, C8600-05, Hamamatsu Photonics, Japan) and acquired with a CCD camera (TC285SPD, Texas Instruments, Texas) or directly acquired with an EMCCD camera (iXon Ultra, Andor, Oxford) at 33-ms intervals. Each single molecule was tracked using homemade software.

2.2. Cell preparations and other methods

Dictyostelium discoideum cells were used for all experiments. Full methods and any associated references are available in the supplementary information.

3. Results

3.1. Three distinct types of G protein dynamics have different cAMP dose dependency

To characterize G protein dynamics over a wide concentration range, we determined EC_{50} for cAR1-mediated activation and translocation by using live imaging analyses. First, fluorescence resonance energy transfer (FRET) between the Gα2 and Gβγ subunits was used to assess cAR1-mediated activation as described previously [19]. Receptor stimulation caused a loss of FRET signals due to dissociation between the two subunits in a dose-dependent manner (Fig. 1A and B, and Video S1). The EC_{50} for the activation was determined to be 2.3 nM with a Hill coefficient of 0.9 (Fig. 1C). The translocation of G protein upon cAMP stimulation was observed by confocal microscopy (Fig. 1D and E, and Video S2) [13,20]. Upon receptor stimulation, cytosolic G protein underwent translocation to the membrane within a few seconds with an EC_{50} of 12 nM and Hill coefficient of 0.8 (Fig. 1C). This translocation was Gip1-dependent and generated a biased localization along the chemoattractant gradients on the membrane, as reported previously [13]. Thus, the G protein activation and translocation could cover the low and middle ranges (<100 nM cAMP), in which the G protein can form intracellular gradients on the membrane along extracellular chemical gradients by its activation and biased translocation. In this scenario, the activated G protein will be saturated with no intracellular gradient at over several hundred nanomolar cAMP if no other mechanism exists.

Supplementary video related to this article can be found at https://doi.org/10.1016/j.bbrc.2018.11.029.

To further examine the G protein dynamics on the membrane, we applied single-molecule imaging to cAR1, Gα2, and Gγ molecules. We prepared *Dictyostelium* cells expressing functional cAR1, Gα2, and Gγ molecules fused to HaloTag (Fig. S1) [21,22]. The Halo-tagged proteins stained with tetramethylrhodamine (TMR) were visualized by total internal reflection fluorescence microscopy (TIRFM). Single molecules of TMR-conjugated cAR1 (cAR1-TMR), Gα2 (Gα2-TMR), and Gγ (Gγ-TMR) were observed on the basal membrane of cells under the same conditions. Upon receptor stimulation with saturating cAMP concentration (10 μM), Gα2-TMR clearly exhibited a mobility shift from a highly mobile state to a slower one (Fig. 1F and Video S3), while cAR1-TMR and Gγ-TMR exhibited no obvious changes in their mobility (Video S3). To characterize the mobility of Gα2-TMR, the diffusion coefficients of individual molecules were determined by short-range diffusion (SRD) analysis as described previously [21] (see Supplementary Material and Methods). The obtained diffusion coefficients of Gα2-TMR exhibited two peaks in the histograms, in which the slower-mobile fraction increased with cAMP concentration (Fig. 1G). The proportion of the slower-mobile fraction in the two diffusion states was determined by probability density function (PDF)-based analysis as described previously [21] (see Supplementary Material and Methods). The fraction of Gα2-TMR in the slower state increased from 20% to 53% across the range of stimuli applied. The results show that the slower-mobile fraction of Gα2-TMR had an EC_{50} of 270 nM and Hill coefficient of 1.0 (Fig. 1C). This dependency coincided with the lower of the known two cAR1 affinities [23].

Supplementary video related to this article can be found at https://doi.org/10.1016/j.bbrc.2018.11.029.

3.2. Complex formation between cAR1 and activated Gα2

We further characterized and compared the mobility of cAR1, Gα2, and Gγ by using SRD and PDF analysis (Fig. 2A and B). Gα2-TMR had a mobility similar to Gγ-TMR, and both subunits moved approximately ten-fold faster than cAR1 in unstimulated cells (Fig. 2A). Upon receptor stimulation with saturating 10 μM cAMP, Gα2-TMR exhibited an increase in the slower-mobile fraction with a diffusion coefficient similar to that of cAR1, while cAR1-TMR and Gγ-TMR showed no significant changes in their mobility (Fig. 2A). The diffusion coefficients of these molecules were determined by PDF analysis (Fig. 2B) and are summarized in Table S1 cAR1-TMR had a diffusion coefficient of 0.017 $\mu m^2/s$ regardless of the cAMP stimulation, consistent with previous reports [14,24]. Gα2-TMR adopted two mobile states with diffusion coefficients of

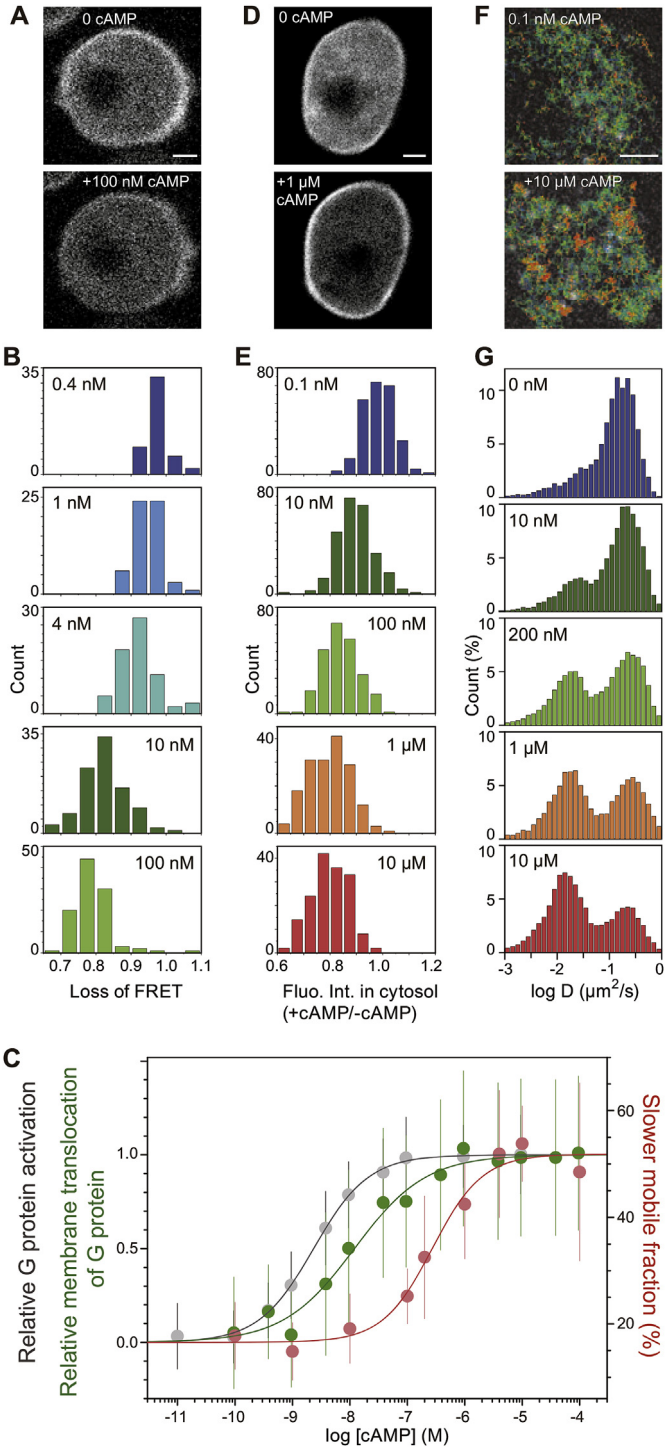

Fig. 1. Three signaling modes in G protein over a wide chemotaxis range. (**A**) G protein activation observed by FRET between the Gα2 and Gβ subunits before and after stimulation. Fluorescence of the FRET acceptor is shown. (**B**) The loss of FRET was measured as an index of the activation for each cell and is shown as histograms at the indicated cAMP concentrations. (**C**) Dose-response curves of the activation (gray), membrane translocation (green), and mobility reduction (red) of Gα2. The equations used for the quantifications are described in Methods. The means ± SD of the analysed cells are plotted. (**D**) G protein localization observed by confocal microscopy before and after stimulation showing translocation to the membrane from the cytosol upon receptor activation. (**E**) Cytosolic fluorescence intensity was measured for each cell and is shown as histograms at the indicated cAMP concentrations. (**F**) Trajectories of single Gα2-TMR molecules in a cell stimulated by the indicated concentration of cAMP. Red and blue indicate slow and fast movement, respectively. (**G**) Histograms of short range diffusion (SRD) coefficients of Gα2-TMR at the indicated cAMP concentrations. Scale bar, 2 μm. (For interpretation of the references to colour in this figure legend, the reader is referred to the Web version of this article.)

0.20–0.22 and 0.015–0.016 $\mu m^2/s$ regardless of the cAMP stimulation (Table S1). The slow-mobile state of Gα2-TMR had the same diffusion coefficient as cAR1-TMR with 95% confidence (Fig. 2B).

One possible explanation for both the cAMP-induced mobility shift of Gα2 and the dose-dependency coinciding with the receptor affinity is that activated Gα2 forms a complex with cAMP-cAR1 complexes. To verify this hypothesis, we examined Gα2 mobility when cAR1 mobility was externally modulated. First, we treated cells with benomyl as reported previously [25]. Consistently, benomyl treatment slowed cAR1-TMR mobility with a diffusion coefficient of 0.003 $\mu m^2/s$ (Fig. 2C). Further, the slower Gα2-TMR fraction in these cells changed its mobility towards that of cAR1 with a diffusion coefficient of 0.005 $\mu m^2/s$ upon cAMP stimulation. Second, cAR1 diffusion was constrained by being tethered to the glass surface (see Supplementary Material and Methods). Concomitant to the immobilization of cAR1, the slower-mobile fraction of Gα2 caused a shift to the immobilized state, consistent with the formation of cAR1-Gα2 complexes (Fig. 2D). The diffusion coefficients of the cAR1 and slower Gα2 fractions were 0.004 $\mu m^2/s$ and 0.005 $\mu m^2/s$, respectively. To further confirm that the activation state of Gα2 is responsible for complex formation with the receptor, we observed a constitutively active Gα2 mutant, Q208L [26]. Gα2(Q208L) showed a slower-mobile fraction even in the absence of cAMP, and this fraction increased with increasing cAMP (Fig. 2E), indicating both G protein activation and receptor occupation with cAMP can promote the complex formation. Thus, chemotactic receptors activate, recruit, and capture the cognate G proteins with half maximum dependencies of 2.3, 12, and 270 nM cAMP, respectively. The capturing of active Gα2 by the occupied receptor can contribute to the spatial retention of the chemotactic signals at the higher ranges.

3.3. cAR1-Gα2 complex formation was correlated with chemotactic range extension

Three different modes in the G protein dynamics can explain the sub-nanomolar to micromolar chemotaxis range of *Dictyostelium* cells. We assume that the complex formation between cAR1 and Gα2 is related to the chemotaxis range extension. To test this hypothesis by extending the dose-dependency of the complex formation to the higher range, we decreased the affinity of cAR1 by using a chimera receptor in which the second extracellular loop (EL2) was replaced with that of cAR2, a low-affinity homolog of cAR1 (cAR1-R2(EL2)) [27]. Single molecules of Gα2-TMR exhibited mobility shifts with an EC_{50} of 1.8 μM and 720 nM in *car1*/*car3* knockout and wild type (WT) cells expressing cAR1-R2(EL2), respectively (Fig. 3A), which is consistent with the complex formation of Gα2 with the occupied receptors. Next, we observed the chemotaxis ability of cAR1-R2(EL2)-expressing cells under high cAMP concentration condition. When a micropipette containing 1 mM cAMP was placed in the dish, cAR1-R2(EL2)-expressing cells reached the tip of the capillary, while WT cells did not gather efficiently around the tip (Fig. 3B and C, and Video S4). Under lower cAMP concentrations, WT cells exhibited efficient chemotaxis [13]. We performed small population assay (see Supplementary Material and Methods) to evaluate the chemotactic efficiency of each cell line and found that cAR1-R2(EL2)-expressing cells extended their sensitivity range to high cAMP concentrations (Fig. 3D). Thus, lowering the affinity of cAR1 caused shifts in the range of chemotaxis and the complex formation between Gα2 and cAR1 to the higher concentration ranges, suggesting spatial retention of the chemotactic signals by the complex formation regulates the sensitivity range.

Supplementary video related to this article can be found at https://doi.org/10.1016/j.bbrc.2018.11.029.

3.4. Complex formation regulated intracellular dynamics of Gα2 along chemical gradients

We next measured the membrane-binding lifetimes of G protein to examine the effects of receptor activation on the membrane-binding stability of G protein (Fig. 4). Single-molecule imaging showed that Gα2-TMR suddenly appeared from the cytosol, subsequently diffused on the membrane, and then suddenly disappeared from the membrane (Video S3). We determined the lifetimes of membrane-bound Gα2-TMR by measuring the duration between the appearance and disappearance of individual molecules (See Supplementary Material and Methods). Gα2-TMR had a lifetime of 1.3 s without cAMP (Fig. 4A), while upon receptor stimulation with uniform 10 μM cAMP, the lifetime was prolonged to ~13.3 s (Fig. 4A). Constitutively active Gα2(Q208L) had lifetimes of 0.7 and 3.4 s without cAMP, but ~26.2 s with cAMP stimulation (Fig. 4B). The obtained value for WT Gα2 is similar to the reported degradation time of Gα-GTP estimated from the interconversions of the cAMP-binding sites [28]. These results indicate that both cAMP-bound receptor and G protein activation were required to stabilize the membrane binding of the Gα2 subunit. We further assessed the mobility and lifetimes of Gα2 under cAMP gradients. Cells expressing Gα2-TMR were stimulated by a double-barreled micropipette with two separate chambers containing either

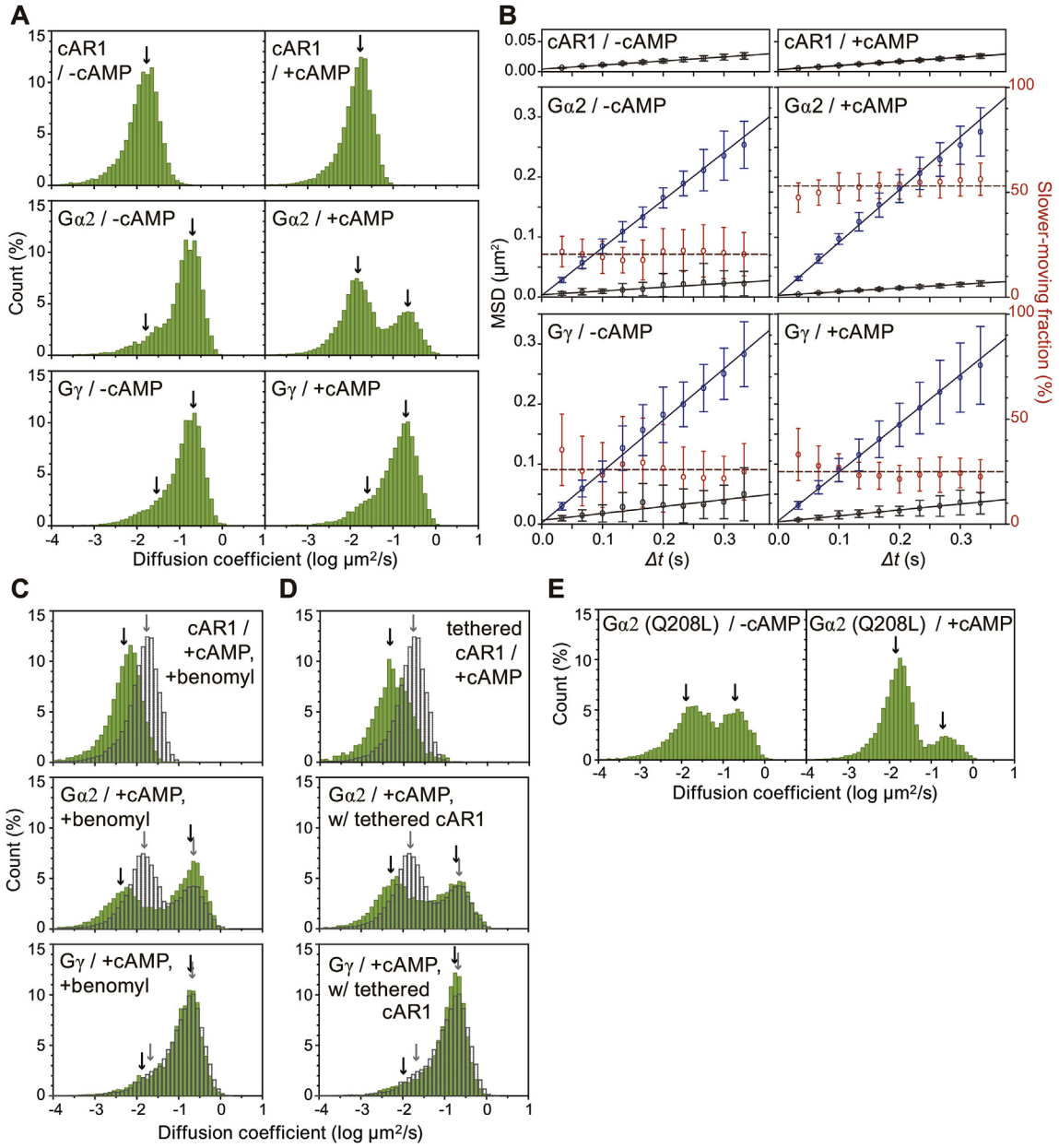

Fig. 2. Complex formation between cAMP receptor cAR1 and activated Gα2 upon their activation. (**A**) Histograms of the SRD coefficients in unstimulated (left) and stimulated (right) cells expressing cAR1-TMR, Gα2-TMR, and Gγ-TMR. (**B**) MSD plots obtained by PDF-based analysis. cAR1-TMR, Gα2-TMR, and Gγ-TMR in the absence (left) or presence (right) of 10 μM cAMP. PDF-based MSD plots of fast (blue) and slow (black) diffusion, and the proportion of the slower fraction (red). The means ± SD of the analysed cells are plotted ($n \geq 9$ cells). (**C and D**) Histograms of the SRD coefficients in cells treated with 100 μM benomyl (C) and cells in which cAR1-TMR was tethered on the glass surface (D). (**E**) Histograms of SRD coefficients of Gα2(Q208L)-TMR observed in unstimulated (left) and stimulated (right) cells. (For interpretation of the references to colour in this figure legend, the reader is referred to the Web version of this article.)

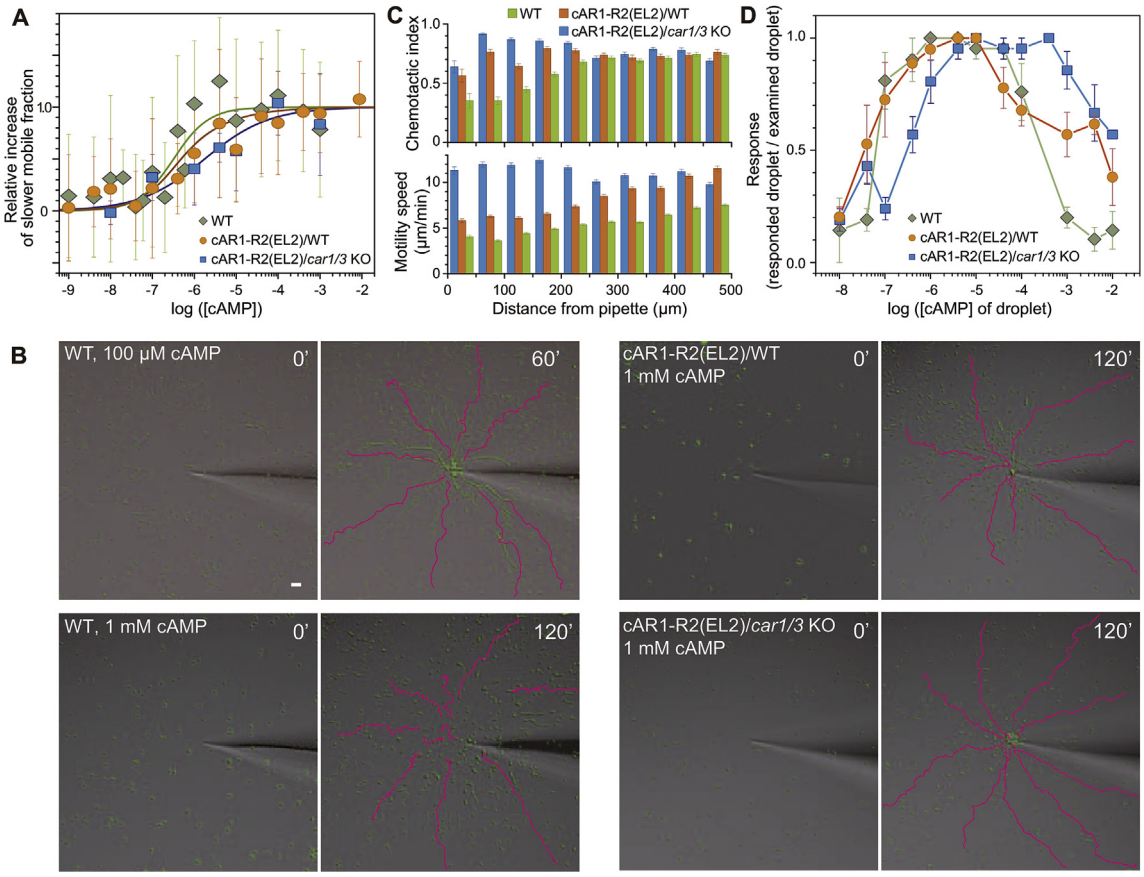

Fig. 3. Shift in cAR1-Gα2 complex formation and chemotaxis range induced by the low-affinity receptor cAR1-R2(EL2). (**A**) Dose-response curve of the slower-mobile fraction of Gα2-TMR obtained from WT (green lozenge), cAR1-R2(EL2)-expressing WT (orange circle), and cAR1-R2(EL2)-expressing cAR1/3 KO (blue square) cells. The means ± SD of individual cells ($n \geq 3$) are shown. (**B**) Micropipette assay of chemotaxis. WT and cAR1-R2(EL2)-expressing cells were stimulated with 100 μM or 1 mM cAMP. The range extension by cAR1-R2(EL2) expression is shown. Cells are highlighted in green. Representative trajectories of cells are shown in magenta. Time, 0 and 60 or 0 and 120 min. (**C**) Chemotactic index (upper) and motility speed (bottom) of >100 trajectories were analysed and are shown as bar graphs (means ± SEM). (**D**) Small population assay of chemotaxis. Data represent the means ± SEM of three experiments. Scale bar, 50 μm. (For interpretation of the references to colour in this figure legend, the reader is referred to the Web version of this article.)

10 nM or 1 μM cAMP (Fig. 4C), and single molecules of Gα2-TMR were visualized (Fig. 4D and Video S5). Gα2-TMR exhibited longer lifetimes with slow mobility in the cell sides facing the higher cAMP concentration than those facing the lower (Fig. 4E and F). Thus, capturing by cAMP receptor prolongs the lifetime of G protein, leading to the generation of intracellular G protein gradients along chemoattractant gradients at higher ranges.

Supplementary video related to this article can be found at https://doi.org/10.1016/j.bbrc.2018.11.029.

4. Discussion

In this report, we found that a chemoattractant triggers three distinct G protein dynamics with different concentration dependencies, and all three types ensure wide-range chemotaxis (Fig. S2). Moreover, our results suggest the known high- and low-affinity states of cAR1 have different roles in G protein regulation. Approximately 10% and 90% of total cAR1 receptors have high affinity (Kd = 3.5–30 nM) and low affinity (Kd = 200–500 nM), respectively [29–32]. That cAMP induced G protein activation with an EC_{50} of 2.3 nM is consistent with the affinity of high-affinity state cAR1, which is likely to be the state responsible for G protein activation [23,33]. Gip1 regulates the spatial distribution of G proteins between the cytosol and the membrane upon ligand stimulation with an EC_{50} of 12 nM. A portion of G proteins is sequestered to the cytosol by binding to Gip1. These cytosolic G proteins are eventually released from Gip1 and change their distribution along the cAMP gradients [13]. The complex between Gα2 and cAR1 appears with an EC_{50} of 270 nM, which is similar to the Kd of low-affinity state receptors. Additionally, an affinity-reducing mutation on cAR1 reduced the value of EC_{50} for the complex formation and also extended the chemotactic dynamic range to higher concentrations. Therefore, the observed G protein dynamics together could cover the whole chemotactic dynamic range of cAMP (sub-nanomolar to several micromolar).

The direct observation of G proteins using single-molecule TIRFM imaging revealed an unconventional stable complex formation with GPCR, represented by the slower mobile population of Gα2. 98% of inactive G protein transiently bound to the membrane with a binding lifetime of about 1 s (Table S1). This homogeneous short membrane binding time suggested that G proteins do not pre-couple with cAR1. Consistently, most G proteins diffused faster than cAR1 in the unstimulated condition. Agonist stimulation initiated receptor-mediated activation of G proteins, although this process was too fast to be observed with our single-molecule imaging system. Because our experimental setup took 33 ms for an image acquisition, GPCR should activate G proteins in less time. This notion is supported by evidence that Gβγ behavior did not change before or after ligand stimulation. On the other hand, the activated Gα2 subunit dissociated from Gβγ to make a complex with the cAR1 receptor on the membrane. This complex formation was indicated by the agonist-induced reduction of the Gα2 diffusion coefficient to

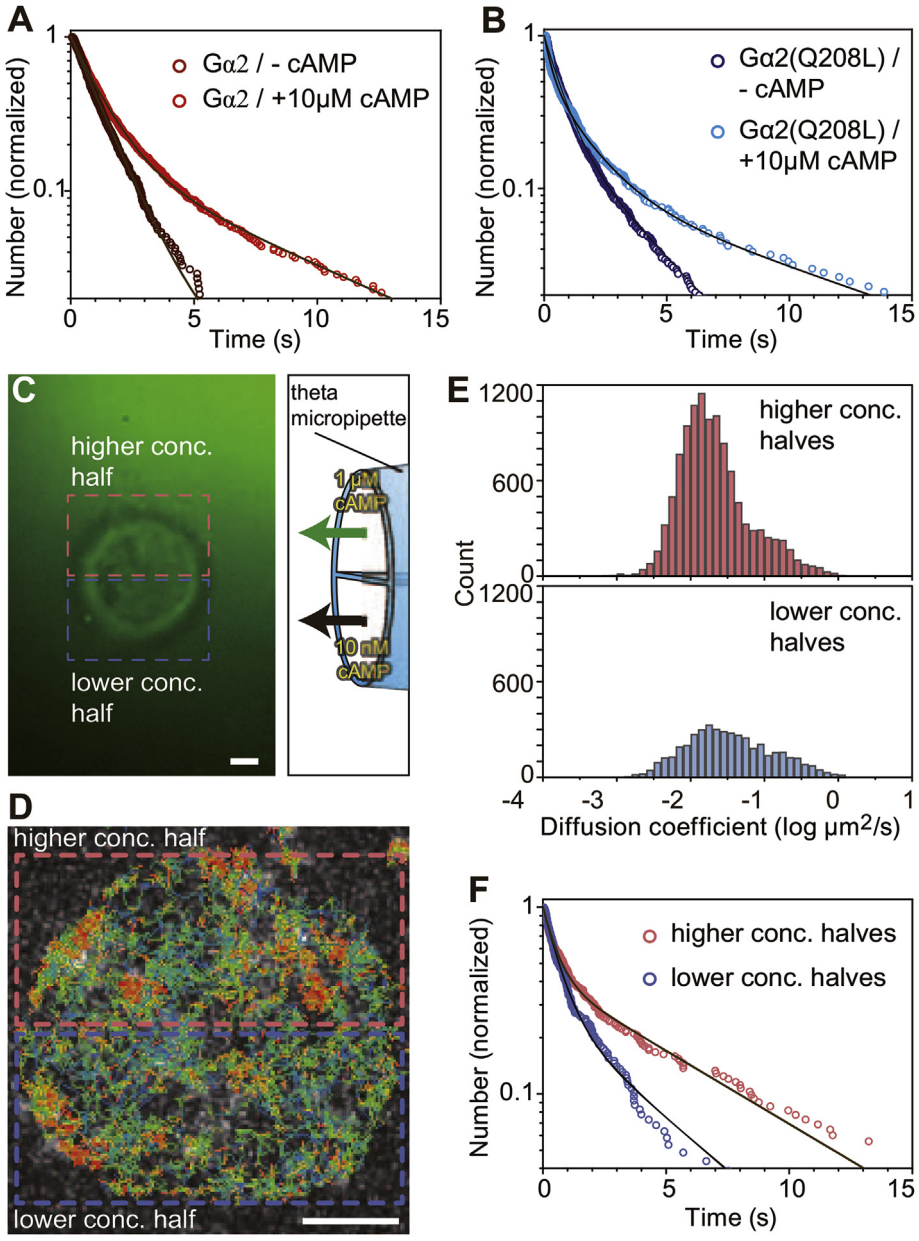

Fig. 4. Complex formation and stabilization of activated Gα2 along chemoattractant gradients. Lifetime analysis of WT Gα2-TMR (**A**) and constitutively active Gα2(Q208L)-TMR (**B**). Solid lines indicate fitting curves of the sum of exponentials (see Supplementary Material and Methods and Table S1). (**C**) Single-molecule analysis of Gα2-TMR under a steep cAMP gradient formed by a theta micropipette with two separate chambers containing either 10 nM or 1 μM cAMP. (**D**) Trajectories of single molecules of Gα2-TMR in a cell exposed to the gradient. (**E and F**) Histograms of SRD coefficients and lifetimes of Gα2-TMR, respectively, observed on the cell halves facing the higher (red) or lower (blue) cAMP concentrations. Scale bar, 2 μm. (For interpretation of the references to colour in this figure legend, the reader is referred to the Web version of this article.)

a rate comparable with the cAR1 diffusion coefficient. Consistently, when receptor diffusion was constrained, the diffusion of Gα2 showed a corresponding reduction. cAR1-Gα2 complex formation increased concomitantly with cAMP occupancy of the low-affinity state cAR1. These results suggest that the ligand-occupied, low-affinity receptors were used as binding sites for the longer membrane lifetime of Gα2. The membrane binding time of Gα2 was 13 s. It was previously reported that the cAMP binding time of low-affinity cAR1 is 1 s [14]. Both values can be explained by the repeated association and dissociation of Gα2 with its neighboring receptors. Altogether, this unconventional complex formation extends the chemotactic dynamic range by producing local information of the receptor occupancy even after all G proteins are already activated.

Because wide sensitivity is a general property of GPCR signaling, the multiple modes of G protein dynamics may be shared with other cell types as a common mechanism, thus providing an additional layer of range regulation in addition to negative feedback on GPCRs.

Acknowledgments

We thank Tatsuo Shibata for development of the PDF-based diffusion analysis methods in the early stage of this work, Masahiro Takahashi for preparing the Gγ gene and knockout cell, National BioResource Project (NBRP)-nenkin for *gα2*⁻ and RI9 cells, DictyBase for basic information on the *Dictyostelium* cells, and Peter Karagiannis for critically reading the manuscript. We also thank all

members of the Ueda laboratory for discussions and technical assistance. This research was partially supported by Japan Society for the Promotion of Science (JSPS) KAKENHI Grant 17K15105 (to Y.M.) and 17K07396 (to Y.K.), and by the Advanced Research and Development Programs for Medical Innovation (AMED-CREST) from Japan Agency for Medical Research and development, AMED JP18gm0910001 (to M.U.).

Appendix A. Supplementary data

Supplementary data to this article can be found online at https://doi.org/10.1016/j.bbrc.2018.11.029.

Transparency document

Transparency document related to this article can be found online at https://doi.org/10.1016/j.bbrc.2018.11.029.

References

[1] D. Koshland, A. Goldbeter, J. Stock, Amplification and adaptation in regulatory and sensory systems, Science (80-.) 217 (1982) 220–225, https://doi.org/10.1126/science.7089556.
[2] O. Hoeller, D. Gong, O.D. Weiner, How to understand and outwit adaptation, Dev. Cell 28 (2014) 607–616, https://doi.org/10.1016/j.devcel.2014.03.009.
[3] S. Asakura, H. Honda, Two-state model for bacterial chemoreceptor proteins. The role of multiple methylation, J. Mol. Biol. 176 (1984) 349–367. http://www.ncbi.nlm.nih.gov/pubmed/6748079.
[4] S.K. Shenoy, R.J. Lefkowitz, β-arrestin-mediated receptor trafficking and signal transduction, Trends Pharmacol. Sci. 32 (2011) 521–533, https://doi.org/10.1016/j.tips.2011.05.002.
[5] A. Sorkin, M. von Zastrow, Endocytosis and signalling: intertwining molecular networks, Nat. Rev. Mol. Cell Biol. 10 (2009) 609–622, https://doi.org/10.1038/nrm2748.
[6] W. Ma, A. Trusina, H. El-Samad, W.A. Lim, C. Tang, Defining network topologies that can achieve biochemical adaptation, Cell 138 (2009) 760–773, https://doi.org/10.1016/j.cell.2009.06.013.
[7] M. Tang, M. Wang, C. Shi, P.A. Iglesias, P.N. Devreotes, C.-H. Huang, Evolutionarily conserved coupling of adaptive and excitable networks mediates eukaryotic chemotaxis, Nat. Commun. 5 (2014) 5175, https://doi.org/10.1038/ncomms6175.
[8] P.R. Fisher, R. Merkl, G. Gerisch, Quantitative analysis of cell motility and chemotaxis in Dictyostelium discoideum by using an image processing system and a novel chemotaxis chamber providing stationary chemical gradients, J. Cell Biol. 108 (1989) 973–984, https://doi.org/10.1083/jcb.108.3.973.
[9] M. Ueda, T. Shibata, Stochastic signal processing and transduction in chemotactic response of eukaryotic cells, Biophys. J. 93 (2007) 11–20, https://doi.org/10.1529/biophysj.106.100263.
[10] Y. Artemenko, T.J. Lampert, P.N. Devreotes, Moving towards a paradigm: common mechanisms of chemotactic signaling in Dictyostelium and mammalian leukocytes, Cell. Mol. Life Sci. 71 (2014) 3711–3747, https://doi.org/10.1007/s00018-014-1638-8.
[11] J.Y. Kim, R.D.M. Soede, P. Schaap, R. Valkema, J.A. Borleis, P.J.M. Van Haastert, P.N. Devreotes, D. Hereld, Phosphorylation of chemoattractant receptors is not essential for chemotaxis or termination of G-protein-mediated responses, J. Biol. Chem. 272 (1997) 27313–27318, https://doi.org/10.1074/jbc.272.43.27313.
[12] Z. Xiao, Y. Yao, Y. Long, P. Devreotes, Desensitization of G-protein-coupled receptors. agonist-induced phosphorylation of the chemoattractant receptor cAR1 lowers its intrinsic affinity for cAMP, J. Biol. Chem. 274 (1999) 1440–1448. http://www.ncbi.nlm.nih.gov/pubmed/9880518.
[13] Y. Kamimura, Y. Miyanaga, M. Ueda, Heterotrimeric G-protein shuttling via Gip1 extends the dynamic range of eukaryotic chemotaxis, Proc. Natl. Acad. Sci. U. S. A. 113 (2016) 4356–4361, https://doi.org/10.1073/pnas.1516767113.
[14] M. Ueda, Y. Sako, T. Tanaka, P. Devreotes, T. Yanagida, Single-molecule analysis of chemotactic signaling in Dictyostelium cells, Science 294 (2001) 864–867, https://doi.org/10.1126/science.1063951.
[15] M. Ueda, Y. Miyanaga, Y. Toshio, Single-molecule analysis of chemotactic signaling mediated by cAMP receptor on living cells, in: T. Haga, S. Takeda (Eds.), G Protein-coupled Recept. Struct. Funct. Ligand Screen, CRC Press, 2005, pp. 197–218.
[16] T. Wazawa, M. Ueda, Total internal reflection fluorescence microscopy in single molecule nanobioscience, Adv. Biochem. Eng. Biotechnol. 95 (2005) 77–106. http://www.ncbi.nlm.nih.gov/pubmed/16080266.
[17] S. Matsuoka, M. Iijima, T.M. Watanabe, H. Kuwayama, T. Yanagida, P.N. Devreotes, M. Ueda, Single-molecule analysis of chemoattractant-stimulated membrane recruitment of a PH-domain-containing protein, J. Cell Sci. 119 (2006) 1071–1079, https://doi.org/10.1242/jcs.02824.
[18] F. Vazquez, S. Matsuoka, W.R. Sellers, T. Yanagida, M. Ueda, P.N. Devreotes, Tumor suppressor PTEN acts through dynamic interaction with the plasma membrane, Proc. Natl. Acad. Sci. U. S. A. 103 (2006) 3633–3638, https://doi.org/10.1073/pnas.0510570103.
[19] C. Janetopoulos, T. Jin, P. Devreotes, Receptor-mediated activation of heterotrimeric G-proteins in living cells, Science 291 (2001) 2408–2411, https://doi.org/10.1126/science.1055835.
[20] C.A. Elzie, J. Colby, M.A. Sammons, C. Janetopoulos, Dynamic localization of G proteins in Dictyostelium discoideum, J. Cell Sci. 122 (2009) 2597–2603, https://doi.org/10.1242/jcs.046300.
[21] Y. Miyanaga, S. Matsuoka, M. Ueda, Single-molecule imaging techniques to visualize chemotactic signaling events on the membrane of living Dictyostelium cells, Methods Mol. Biol. 571 (2009) 417–435, https://doi.org/10.1007/978-1-60761-198-1_28.
[22] S. Matsuoka, Y. Miyanaga, M. Ueda, Multi-state transition kinetics of intracellular signaling molecules by single-molecule imaging analysis, Methods Mol. Biol. 1407 (2016) 361–379, https://doi.org/10.1007/978-1-4939-3480-5_25.
[23] P.M. Janssens, P.J. Van Haastert, Molecular basis of transmembrane signal transduction in Dictyostelium discoideum, Microbiol. Rev. 51 (1987) 396–418.
[24] Y. Miyanaga, S. Matsuoka, T. Yanagida, M. Ueda, Stochastic signal inputs for chemotactic response in Dictyostelium cells revealed by single molecule imaging techniques, Biosystems 88 (2007) 251–260, https://doi.org/10.1016/j.biosystems.2006.07.011.
[25] S. De Keijzer, J. Galloway, G.S. Harms, P.N. Devreotes, P.A. Iglesias, Disrupting microtubule network immobilizes amoeboid chemotactic receptor in the plasma membrane, Biochim. Biophys. Acta Biomembr. 1808 (2011) 1701–1708, https://doi.org/10.1016/j.bbamem.2011.02.009.
[26] K. Okaichi, A.B. Cubitt, G.S. Pitt, R.A. Firtel, Amino acid substitutions in the Dictyostelium G alpha subunit G alpha 2 produce dominant negative phenotypes and inhibit the activation of adenylyl cyclase, guanylyl cyclase, and phospholipase C, Mol. Biol. Cell 3 (1992) 735–747. http://www.ncbi.nlm.nih.gov/pubmed/1355376.
[27] J.Y. Kim, J.A. Borleis, P.N. Devreotes, Switching of chemoattractant receptors programs development and morphogenesis in Dictyostelium: receptor subtypes activate common responses at different agonist concentrations, Dev. Biol. 197 (1998) 117–128, https://doi.org/10.1006/dbio.1998.8882.
[28] P.J.M. van Haastert, R.J.W. de Wit, P.M.W. Janssens, F. Kesbeke, J. DeGoede, G-protein-mediated interconversions of cell-surface cAMP receptors and their involvement in excitation and desensitization of guanylate cyclase in Dictyostelium discoideum, J. Biol. Chem. 261 (1986) 6904–6911.
[29] R.L. Johnson, M.J. Caterina, P.N. Devreotes, P.J.M. Van Haastert, R.A. Vaughan, Overexpression of the cAMP receptor 1 in growing Dictyostelium cells, Biochemistry 30 (1991) 6982–6986, https://doi.org/10.1021/bi00242a025.
[30] P.J.M. Van Haastert, J.D. Bishop, R.H. Gomer, The cell density factor CMF regulates the chemoattractant receptor cAR1 in Dictyostelium, J. Cell Biol. 134 (1996) 1543–1549, https://doi.org/10.1083/jcb.134.6.1543.
[31] J.L.S. Milne, M.J. Caterina, P.N. Devreotes, Random Mutagenesis of the cAMP Chemoattractant Receptor , cAR1 , of Dictyostelium, vol. 272, 1997, pp. 2069–2076.
[32] M. Zhang, Constitutively active G protein-coupled receptor mutants block Dictyostelium development, Mol. Biol. Cell 16 (2005) 562–572, https://doi.org/10.1091/mbc.E04-06-0456.
[33] A. De Lean, J.M. Stadel, R.J. Lefkowitz, A ternary complex model explains the agonist-specific binding properties of the adenylate cyclase-coupled β-adrenergic receptor, J. Biol. Chem. 255 (1980) 7108–7117, doi:1809.